Princeton Plasma Physics Laboratory

PPPL- 4853

PPPL- 4853

Guiding Center Equations for Ideal Magnetohydrodynamic Modes

Roscoe B. White

February, 2013

PPPL PRINCETON PLASMA PHYSICS LABORATORY

Prepared for the U.S. Department of Energy under Contract DE-AC02-09CH11466.

Princeton Plasma Physics Laboratory
Report Disclaimers

Full Legal Disclaimer

Trademark Disclaimer

PPPL Report Availability

Princeton Plasma Physics Laboratory:

http://www.pppl.gov/techreports.cfm

Office of Scientific and Technical Information (OSTI):

http://www.osti.gov/bridge

Related Links:

U.S. Department of Energy

Office of Scientific and Technical Information

Fusion Links

latex /Compute/Lagrange/fullxi.tex

Guiding Center Equations for Ideal Magnetohydrodynamic Modes

R. B. White[1]

[1]*Plasma Physics Laboratory, Princeton University,*

P.O.Box 451, Princeton, New Jersey 08543

Abstract

Guiding center simulations are routinely used for the discovery of mode-particle resonances in tokamaks, for both resistive and ideal instabilities and to find modifications of particle distributions caused by a given spectrum of modes, including large scale avalanches during events with a number of large amplitude modes. One of the most fundamental properties of ideal magnetohydrodynamics is the condition that plasma motion cannot change magnetic topology. The conventional representation of ideal magnetohydrodynamic modes by perturbing a toroidal equilibrium field through $\delta\vec{B} = \nabla \times (\vec{\xi} \times \vec{B})$ however perturbs the magnetic topology, introducing extraneous magnetic islands in the field. A proper treatment of an ideal perturbation involves a full Lagrangian displacement of the field due to the perturbation and conserves magnetic topology as it should. In order to examine the effect of ideal magnetohydrodynamic modes on particle trajectories the guiding center equations should include a correct Lagrangian treatment. Guiding center equations for an ideal displacement $\vec{\xi}$ are derived which perserve the magnetic topology and are used to examine mode particle resonances in toroidal confinement devices. These simulations are compared to others which are identical in all respects except that they use the linear representation for the field. Unlike the case for the magnetic field, the use of the linear field perturbation in the guiding center equations does not result in extraneous mode particle resonances.

PACS numbers: 52.35.Bj, 52.35.Vd

I. INTRODUCTION

Guiding center codes are routinely used to simulate the modification of particle distributions in fusion devices caused by a spectrum of unstable modes, including toroidal Alfvén eigenmodes and other kinetic instabilities excited by a high energy particle population such as an injected beam used for heating or thermonuclearly produced alpha particles[1–3].

A representation of the magnetic field perturbation which is linear in the ideal displacement $\vec{\xi}$ does not preserve magnetic topology[4], creating magnetic islands which should not be present, although unlikely to modify stability or growth rate calculations because the islands occupy a fraction of the total plasma volume proportional to the ideal displacement ξ, and the perturbed energy is proportional to ξ^2, so the correction to the energy should be of order ξ^3. Unlike the calculation of plasma stability however, the modification of particle distributions is caused by locally occuring resonances, and the total change in the distribution is due to the number and size of these resonances, so the occurance of extraneous resonances could be important. In this work we investigate whether the linear treatment of the field perturbation also introduces extraneous mode-particle resonances which could compromise the analysis of the effect of the modes on particle distributions. In order to correctly find the effect of ideal modes on particle distributions one must find the equations of motion using a full Lagrangian treatment of the field produced by the ideal displacement $\vec{\xi}$.

The equilibrium field in a toroidal axisymmetric equilibrium has covariant and contravariant representations, given by $\vec{B}_0 = \nabla\zeta \times \nabla\psi_p + q\nabla\psi_p \times \nabla\theta = g\nabla\zeta + I\nabla\theta + \delta\nabla\psi_p$ with $q(\psi_p)$ the field line helicity, ψ_p the poloidal flux, θ and ζ poloidal and toroidal coordinates and ψ_p, θ, and ζ forming a right handed coordinate system with Jacobian $1/\mathcal{J}_p = \nabla\psi_p \cdot (\nabla\theta \times \nabla\zeta)$. The toroidal flux is ψ with $d\psi = q(\psi_p)d\psi_p$. The function g is a flux function, and we use Boozer coordinates[5] with $I = I(\psi_p)$. Contravariant bases for the coordinate system are given by $\vec{e}^{\beta} = \nabla\beta$ with $\beta = \psi_p$, θ, and ζ[6]. A magnetohydrodynamic (MHD) instability is given by the plasma displacement $\vec{\xi}$, producing a modification of the magnetic field, with linear representation $\delta\vec{B} = \nabla \times (\vec{\xi} \times \vec{B})$.

In section II we find guiding center equations using the linear representation for the field perturbation $\delta\vec{B} = \nabla \times (\vec{\xi} \times \vec{B})$ and explore the mode particle resonances produced by typical perturbations. In section III we find the modified guiding center equations using the

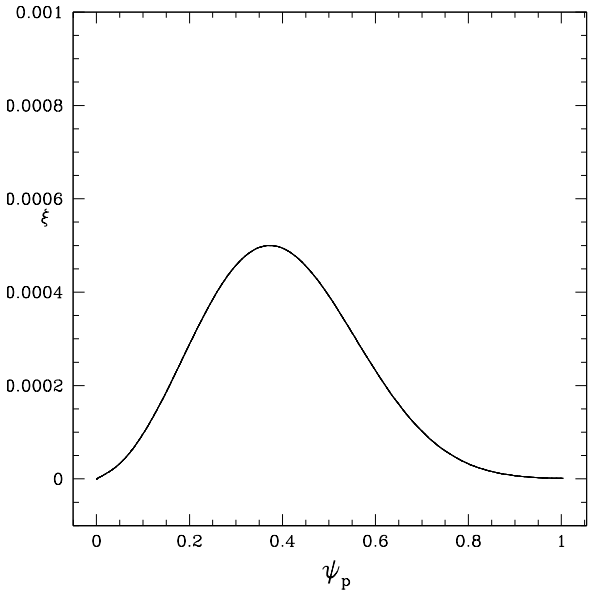

FIG. 1: The radial dependence of the harmonics for ξ^{ψ_p} used for the development and examination of the guiding center equations.

full Lagrangian displacement representation for the field perturbation and compare these results with those obtained using the linear representation of the field. In section IV are the conclusions.

II. LINEAR PERTURBATION $\delta\vec{B} = \nabla \times (\vec{\xi} \times \vec{B})$

Introduce an ideal perturbation with fluid displacement $\vec{\xi}$ giving a magnetic field perturbation linear in ξ of the form $\delta\vec{B} = \nabla\times(\vec{\xi}\times\vec{B})$. Now expand $\vec{\xi}$ in the covariant basis $\vec{\xi} = \xi^\alpha \vec{e}_\alpha$, and make a Fourier decomposition of $\vec{\xi}$ through $\xi^\psi = \sum_{mn} \xi^\psi_{mn} sin(Q)$, $\xi^\theta = \sum_{mn} \xi^\theta_{mn} cos(Q)$, and $\xi^\zeta = \sum_{mn} \xi^\zeta_{mn} cos(Q)$ with $Q = n\zeta - m\theta - \omega t$ and $\nabla \cdot \vec{\xi} = \frac{1}{\mathcal{J}_p}\partial_\alpha(\mathcal{J}_p \xi^\alpha)$. In Fig. 1 is shown a sample global harmonic for the representation of the displacements ξ^{ψ_p}, ξ^θ, ξ^ζ used for the development and verification of the guiding center equations.

Write the guiding center Lagrangian for a charged particle in a magnetic field[6, 7]

$$L = (\vec{A} + \rho_\parallel \vec{B}) \cdot \vec{v} - H \tag{1}$$

with $\rho_\parallel = v_\parallel / B$, $\vec{A}$ the vector potential, $\vec{v}$ the particle velocity, and H the Hamiltonian

$$H = \frac{\rho_\parallel^2 B^2}{2} + \mu B + \Phi \tag{2}$$

with μ the magnetic moment and Φ the electric potential. The equilibrium vector potential is $\vec{A} = \psi\nabla\theta - \psi_p\nabla\zeta$ and the perturbation $\delta\vec{A} = \vec{\xi}\times\vec{B}$. Then $\vec{\xi}\times\vec{B} = \xi^\alpha B^\beta \epsilon_{\alpha\beta\gamma}\mathcal{J}_p\vec{e}^\gamma$. The Lagrangian becomes

$$L = (\psi\vec{e}^\theta - \psi_p\vec{e}^\zeta + \xi^\alpha B^\beta\epsilon_{\alpha\beta\gamma}\mathcal{J}_p\vec{e}^\gamma + \rho_\parallel B_\alpha\vec{e}^\alpha)\cdot\vec{v} - H. \tag{3}$$

Using $B^{\psi_p} = 0$, $B^\theta = 1/\mathcal{J}_p$, $B^\zeta = q/\mathcal{J}_p$ this simplifies to

$$L = (\psi + \rho_\parallel I - q\xi^{\psi_p})\dot{\theta} + (\rho_\parallel g - \psi_p + \xi^{\psi_p})\dot{\zeta} + (q\xi^\theta - \xi^\zeta)\dot{\psi}_p - H \tag{4}$$

where we have dropped δ, not modifying the particle trajectory in the poloidal plane and giving rise only to periodic oscillations in the toroidal precession.

Largange's equations are

$$\frac{d}{dt}\frac{\partial L}{\partial\dot{q}} = \frac{\partial L}{\partial q} \tag{5}$$

giving

$$\begin{pmatrix} 0 & -A & -C & 0 \\ A & 0 & -F & I \\ C & F & 0 & g \\ 0 & -I & -g & 0 \end{pmatrix}\begin{pmatrix} \dot{\psi}_p \\ \dot{\theta} \\ \dot{\zeta} \\ \dot{\rho}_\parallel \end{pmatrix} = \begin{pmatrix} -\partial_{\psi_p}H - q\partial_t\xi^\theta + \partial_t\xi^\zeta \\ -\partial_\theta H + q\partial_t\xi^{\psi_p} \\ -\partial_\zeta H - \partial_t\xi^{\psi_p} \\ -\partial_{\rho_\parallel}H \end{pmatrix} \tag{6}$$

with

$$\begin{aligned} A &= q + \rho_\parallel I' - \partial_{\psi_p}(q\xi^{\psi_p}) - q\partial_\theta\xi^\theta + \partial_\theta\xi^\zeta \\ C &= \rho_\parallel g' - 1 + \partial_{\psi_p}\xi^{\psi_p} - q\partial_\zeta\xi^\theta + \partial_\zeta\xi^\zeta \\ F &= \partial_\theta\xi^{\psi_p} + q\partial_\zeta\xi^{\psi_p} \end{aligned} \tag{7}$$

which we invert to find

$$\begin{pmatrix} \dot{\psi}_p \\ \dot{\theta} \\ \dot{\zeta} \\ \dot{\rho}_\parallel \end{pmatrix} = \frac{1}{Ag - IC}\begin{pmatrix} 0 & g & -I & -F \\ -g & 0 & 0 & C \\ I & 0 & 0 & -A \\ F & -C & A & 0 \end{pmatrix}\begin{pmatrix} -\partial_{\psi_p}H - q\partial_t\xi^\theta + \partial_t\xi^\zeta \\ -\partial_\theta H + q\partial_t\xi^{\psi_p} \\ -\partial_\zeta H - \partial_t\xi^{\psi_p} \\ -\partial_{\rho_\parallel}H \end{pmatrix}. \tag{8}$$

The antisymmetry of the matrix giving the time derivatives guarantees energy conservation in the absense of explicit time dependence. From

$$\frac{dH}{dt} = \partial_{\psi_p}H\dot{\psi}_p + \partial_\theta H\dot{\theta} + \partial_\zeta H\dot{\zeta} + \partial_{\rho_\parallel}H\dot{\rho}_\parallel \tag{9}$$

we note that terms cancel one other due to this antisymmetry.

Significant tests of a numerical code for following particle trajectories in a toroidal confinement device consist of Poincaré plots and the observation of energy conservation. Poincaré plots using very low energy particles with zero magnetic moment and zero mode frequency show detailed structure of the magnetic field, very sensitive to numerical errors. Kinetic Poincaré plots indicate mode-particle resonances and the island structure of these resonances is also very sensitive to numerical error. If the mode has zero frequency, then energy conservation is a very sensitive test of the numeral integration scheme and if high energy particles are used energy conservation tests also the correctness of the second order drift terms. Another test is the fact that in the presence of a single mode, since $H = H(n\zeta - \omega t)$

$$\omega \dot{P}_\zeta = n \partial_t H. \tag{10}$$

This condition restricts the motion of particles in the P_ζ, E plane due to the action of a mode.

In Fig. 2 is shown a Poincaré plot of the magnetic field showing the islands produced by the use of a linear representation of a large ideal perturbation. As shown in a previous publication[4] this representation produces unwanted resonance islands near the rational surface $q = m/n$, shown in the figure with a red line, which have width which is linear in the perturbation amplitude.

A kinetic Poincaré plot provides a means of examining mode particle resonances. Points are plotted in the poloidal cross section whenever $n\zeta - \omega_n t = 2\pi k$ with k integer. The toroidal motion then gives successive Poincaré points in the poloidal cross section ψ_p, θ, or better, since P_ζ and E are constant in the absence of perturbations, the P_ζ, θ plane. Individual modes produce islands in the phase space of the particle orbits, which through phase mixing produce local flattening of the particle distribution. In addition, overlap of these islands, the Chirikov criterion, leads to stochastic transport of particles. Such a plot shows the canonical division of orbits into those following good Kolmogorov, Arnold, Moser [10] (KAM) surfaces, isolated islands bounded by separatrices, and stochastic domains. In an ideal situation with a single perturbation the separatrix is a well defined boundary, but in an actual equilibrium it is broadened into a thin stochastic layer by toroidal coupling or nonlinear coupling to other perturbations.

A general method for numerically determining the existence of or the destruction of good

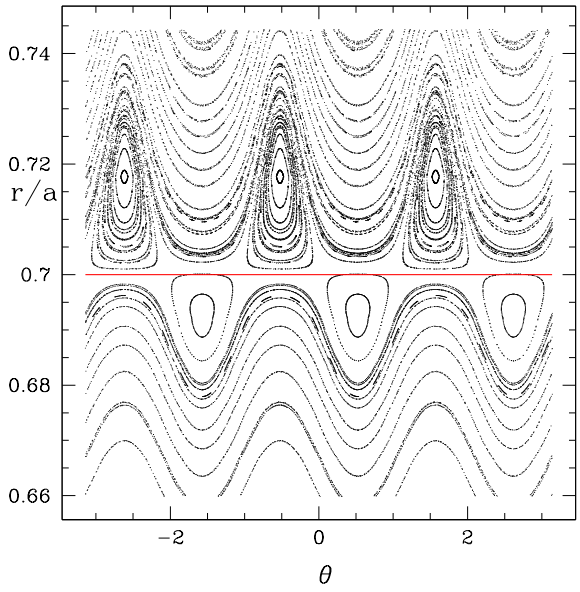

FIG. 2: A Poincaré plot using the linear $\nabla \times (\vec{\xi} \times \vec{B})$ for a zero frequency $m/n = 3/2$ perturbation, showing the extraneous islands produced near the rational surface r/a = 0.7. A large perturbation with $\xi = 3 \times 10^{-3}$ was used.

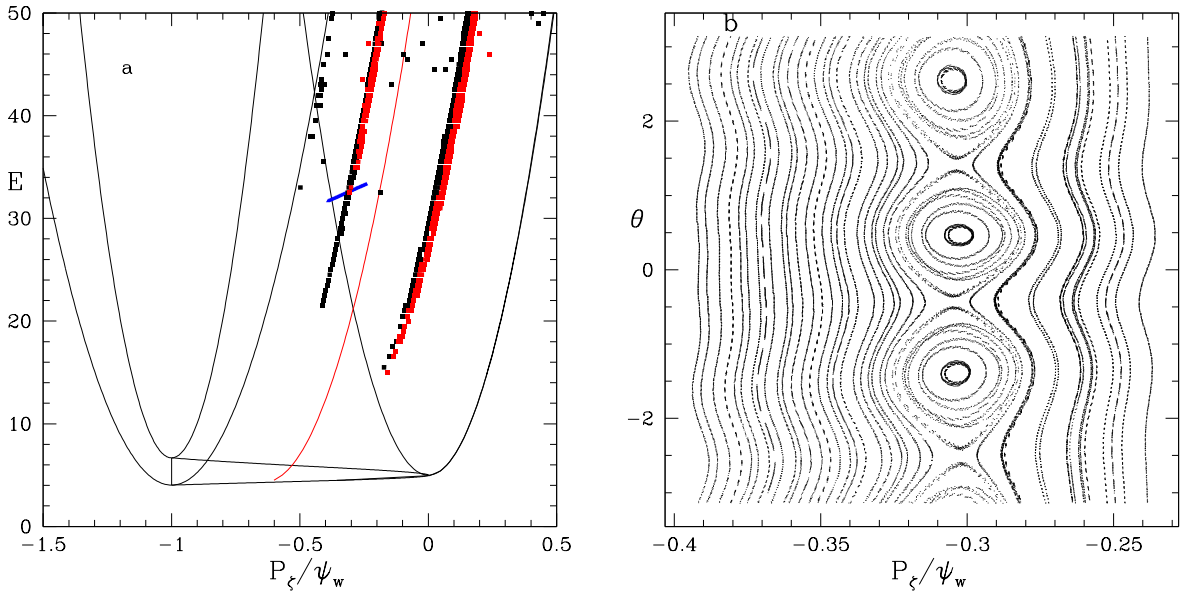

FIG. 3: Resonances in the P_ζ, E plane (a) and a kinetic Poincaré plot (b) using the linear perturbation representation $\nabla \times (\vec{\xi} \times \vec{B})$. A perturbation of magnitude $\xi = 4 \times 10^{-4}$ was used, typical for toroidal Alfvén modes.

KAM surfaces can be obtained using the method of phase vector rotation [8, 9]. Consider following two orbits located nearby one another. Examine a Poincaré section in P_ζ, θ and define the angle χ to give the orientation of the vector joining them in this plane. If good KAM surfaces exist χ can change by at most an angle of π, due to their relative velocity in the angular coordinate. However two orbits within an island rotate around one another with χ increasing with the rotation time abo ut the island O-point giving the bounce frequency of a particle trapped in the wave.

In Fig. 3 is an example of the use of phase vector rotation to find all resonances for a given value of μ. Shown is the P_ζ, E plane, (a) with the locations of resonances marked. Black indicates energy transfer from the particles to the mode, and red the opposite. There are two principle resonance chains, extending over a large range of energy. The mode had a frequency of 40 KHz and mode numbers of $m/n = 3/2$. Also shown with a thin red line is the resonance surface $q = m/n$, where extraneous islands appear in the magnetic field due to the use of the linearized form of the perturbed field. This plot is obtained by launching a large number of pairs of particles, all orbits with magnetic moment $\mu B = 4KeV$, phase vector rotation indicating the presence of a resonance. Also shown (b) is a Poincaré plot obtained along the sloping line in (a) crossing the resonance at the left starting at 32 KeV. This line satisfies $\omega \dot{P}_\zeta = n\partial_t H$, and particle motion induced by the mode takes place along this line. There are no resonances observed in the vicinity of the surface $q = m/n$. Note also that the mode particle resonances observed are much larger than the extraneous islands produced in the magnetic field.

We point out also that simulations have been made with different amplitudes of ξ^θ and ξ^ζ with no discernable modification of resonance location or width. The resonances are entirely determined by the amplitude of the cross field component ξ^{ψ_p}.

III. FULL LAGRANGIAN REPRESENTATION OF THE PERTURBATION

To avoid the production of islands in the magnetic field near the rational surfaces use the ideal MHD condition that the field is frozen into the plasma. Use the Lundquist identity[11, 12]

$$\vec{B}(\vec{r}, t) = \vec{B}_0(\vec{r}_0, 0) + (\vec{B}_0(\vec{r}_0, 0) \cdot \nabla_0)\vec{\xi}(\vec{r}_0, t), \tag{11}$$

where $\vec{r} = \vec{r}_0 + \vec{\xi}$. Thus the field at point $\vec{r}$ is given by the field at the point $\vec{r}_0 = \vec{r} - \vec{\xi}$, *ie* the field has been carried along with the displacement $\vec{\xi}$ in a Lagrangian sense. We then calculate the magnetic field using shifted coordinates, $B(\psi_p - \xi^{\psi_p}, \theta - \xi^{\theta}, \zeta - \xi^{\zeta})$ and then find equations for the step in time.

Thus we wish to find equations of motion using the field evaluated at the point $\vec{r}_0 = \vec{r} - \vec{\xi}$. Write the Lagrangian for the coordinates of $\vec{r}_0$, which we donote by ψ_{p0}, θ_0, ζ_0, giving from Eq. 4

$$L = (\psi_0 + \rho_{\|0} I)\dot{\theta}_0 + (\rho_{\|0} g - \psi_{p0})\dot{\zeta}_0 - H(\psi_{p0}, \theta_0, \zeta_0, \rho_{\|0}) \tag{12}$$

where all functions defining $\vec{B}$, *ie* g, I, q are evaluated at $\vec{r}_0$.

The equations of motion for ψ_{p0}, θ_0, ζ_0, $\rho_{\|0}$ given by this Lagrangian are

$$\begin{pmatrix} 0 & -A & -C & 0 \\ A & 0 & 0 & I \\ C & 0 & 0 & g \\ 0 & -I & -g & 0 \end{pmatrix} \begin{pmatrix} \dot{\psi}_{p0} \\ \dot{\theta}_0 \\ \dot{\zeta}_0 \\ \dot{\rho}_{\|0} \end{pmatrix} = \begin{pmatrix} -\partial_{\psi_{p0}} H \\ -\partial_{\theta_0} H \\ -\partial_{\zeta_0} H \\ -\partial_{\rho_{\|0}} H \end{pmatrix} \tag{13}$$

with $A = q + \rho_{\|} I'$, $C = \rho_{\|} g' - 1$, which we invert to find

$$\begin{pmatrix} \dot{\psi}_{p0} \\ \dot{\theta}_0 \\ \dot{\zeta}_0 \\ \dot{\rho}_{\|0} \end{pmatrix} = \frac{1}{Ag - IC} \begin{pmatrix} 0 & g & -I & 0 \\ -g & 0 & 0 & C \\ I & 0 & 0 & -A \\ 0 & -C & A & 0 \end{pmatrix} \begin{pmatrix} -\partial_{\psi_{p0}} H \\ -\partial_{\theta_0} H \\ -\partial_{\zeta_0} H \\ -\partial_{\rho_{\|0}} H \end{pmatrix} \tag{14}$$

Now return to the particle coordinates ψ_p, θ, ζ. We easily find $\dot{\psi}_p = \dot{\psi}_{p0} + \dot{\xi}^{\psi_p}$, $\dot{\theta} = \dot{\theta}_0 + \dot{\xi}^{\theta}$, $\dot{\zeta} = \dot{\zeta}_0 + \dot{\xi}^{\zeta}$. In the absense of a perturbation we have $\dot{\rho}_{\|} = \dot{\rho}_{\|0}$ but with the perturbation the relation is not trivial because the change in the magnitude of the field requires a change in $\rho_{\|}$. To find $\dot{\rho}_{\|}$ in the presence of a perturbation use $\omega \dot{P}_{\zeta} = n\dot{H}$. We have

$$\frac{dH}{dt} = \rho_{\|} B^2 \frac{d\rho_{\|}}{dt} + \frac{\partial H}{\partial \beta} \frac{d\beta}{dt} \tag{15}$$

where summation over $\beta = \psi_p, \theta, \zeta$ is understood. Then from the Lagrangian Eq. 12 find $P_{\zeta} = g\rho_{\|} - \psi_p + \xi^{\psi_p}$, giving

$$\frac{d\rho_{\|}}{dt} = \frac{n(\partial H/\partial \beta) d\beta/dt + \omega(1 - g')\dot{\psi}_p - \omega \dot{\xi}^{\psi_p}}{\omega g - n\rho_{\|} B^2}. \tag{16}$$

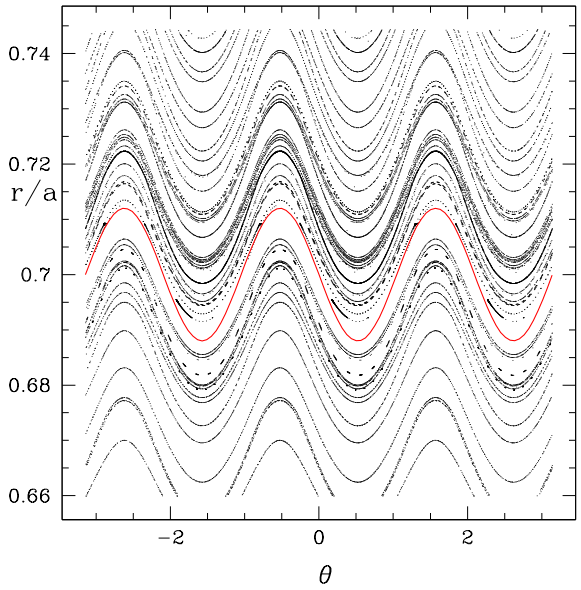

FIG. 4: A Poincaré plot of the magnetic field using the full nonlinear Lundquist expression for following orbits. The red line is the displaced rational surface $q = m/n$. A perturbation of magnitude $\xi = 3 \times 10^{-3}$ was used.

In Fig. 4 is shown the Poincaré plot of the field with the same perturbation present as in Fig. 2. The red line indicates the displaced rational surface $q = m/n$ and of course the field is given by a full Lagrangian displacement, including all orders of ξ, and includes no extraneous islands.

In Fig. 5 is an example of the use of phase vector rotation to find all resonances for a given value of μ, with the same parameters as used for Fig. 3. Shown is the P_ζ, E plane, (a) with the locations of resonances marked. The two principle resonance chains, extending over a large range of energy are the same as shown in Fig. 3. Also shown with a thin red line is the resonance surface $q = m/n$. A Poincaré plot (b) was obtained along the sloping line in (a) crossing the resonance at the left starting at 32 KeV.

A number of such cases have been examined with different mode frequencies and different values of magnetic moment μ, without discovering any extraneous resonances due to the use of the linearized form of the perturbed magnetic field. In particular, no resonances have been observed in the vicinity of the rational surface $q = m/n$.

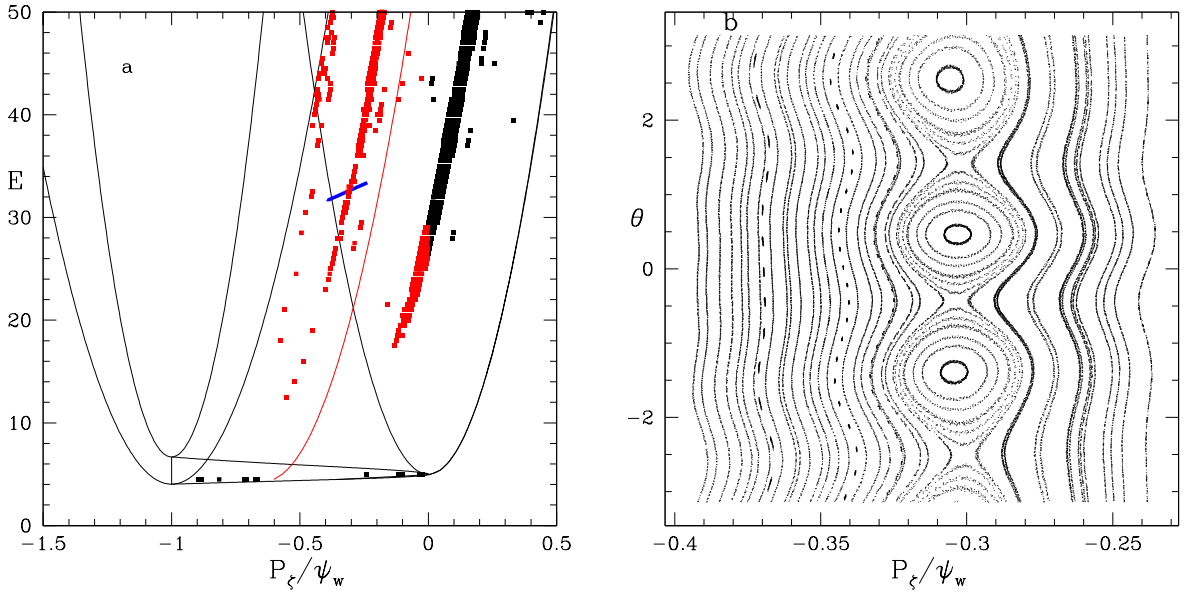

FIG. 5: Resonances in the P_ζ, E plane (a) and a kinetic Poincaré plot (b) using the full Lagrangian representation for the field. A perturbation of magnitude $\xi = 4\times10^{-4}$ was used, typical for toroidal Alfvén modes.

IV. CONCLUSION

Guiding center equations are constructed for ideal MHD modes using both the representation of the field perturbation linear in $\vec{\xi}$ and using the full Lagrangian displacement to find the field perturbation. No modification of the mode-particle resonance spectrum due to the use of the linearized perturbation has been discovered. The particle resonances observed are much larger than the size of the extraneous islands produced in the field, which are linear in ξ, so probably particle drift makes it impossible for these small islands to produce any resonances in the particle dynamics.

Both in the case of linear $\delta\vec{B} = \nabla\times(\vec{\xi}\times\vec{B})$ and with the full Lagrangian displacement the size and location of the resonances is completely independent of the magnitudes of ξ^θ and ξ^ζ, it is only the cross field component of $\vec{\xi}$ that is relevant for mode-particle resonance. This confirms the expectation that mode particle resonances with ideal modes can be safely investigated using the representation $\nabla\times\alpha\vec{B}$ shown to correctly give[4] the cross field component of $\vec{\xi}$.

Acknowledgement The author gratefully acknowledges conversations with Guo-Yong

Fu and other physicists at the Princeton Plasma Physics Laboratory. This work was partially supported by the U.S. Department of Energy Grant DE-AC02-09CH11466.

---

[1] White, R. B., N. N. Gorelenkov, W. W. Heidbrink, M. A. Van Zeeland, *Phys. of Plasmas* **17** 056107 (2010)

[2] White, R. B., N. N. Gorelenkov, W. W. Heidbrink, M. A. Van Zeeland, *Plasmas Physics Controlled Fusion* **52** 045012 (2010)

[3] Gorelenkov N. N. and R. B. White, Plasma Phys Controlled Fusion 55 015007 (2013)

[4] White, R. B. Phys. Plasmas 20, 022105 (2013)

[5] Boozer, A. H., Phys. Fluids 24, 1999 (1981).

[6] White, R. B. *The Theory of Toroidally Confined Plasmas, revised second edition*, Imperial College Press, p. 73 (2006)

[7] Littlejohn, R. Phys. Fluids 24, 1730 (1981), J. Plasma Phys. 29, 111 (1983),

[8] White, R. B. Commun. Nonlin. Sci. Numer. Simulation CNSNS1906 (2011)

[9] White, R. B. Plasma Physics and Controlled Fusion, 53 (2011) 085018

[10] Kolmogorov, A. N. *Proc. Int. Congr. Mathematicians, Amsterdam, Vol 1* 315 (1957), V. I. Arnold, *Russ. Math. Surv.* 18(5):9, 1963, J. Moser, *Math. Phys. Kl. II 1,1 Kl(1):1*, 1962.

[11] Lundquist S., Phys. Rev. 83, 307 (1951)

[12] Roberts, P. H., *Introduction to Magnetohydrodynamics*, p46, Longmans Green, London (1967).

The Princeton Plasma Physics Laboratory is operated
by Princeton University under contract
with the U.S. Department of Energy.

Information Services
Princeton Plasma Physics Laboratory
P.O. Box 451
Princeton, NJ 08543

Phone: 609-243-2245
Fax: 609-243-2751
e-mail: pppl_info@pppl.gov
Internet Address: http://www.pppl.gov